

Antiferro quadrupolar ordering in Fe intercalated few layers graphene



Abu Jahid Akhtar, Abhisek Gupta, Dipankar Chakravorty, and Shyamal K. Saha

Citation: *AIP Advances* **3**, 072124 (2013); doi: 10.1063/1.4816791

View online: <http://dx.doi.org/10.1063/1.4816791>

View Table of Contents: <http://scitation.aip.org/content/aip/journal/adva/3/7?ver=pdfcov>

Published by the *AIP Publishing*



Special Topic: Physics in China
A focus of materials physics research
Enge Wang,, Xincheng Xie, Qikun Xue, Guest Editors

Antiferro quadrupolar ordering in Fe intercalated few layers graphene

Abu Jahid Akhtar,¹ Abhisek Gupta,¹ Dipankar Chakravorty,²
 and Shyamal K. Saha^{1,a}

¹Department of Materials Science, Indian Association for the Cultivation of Science,
 Jadavpur, Kolkata 700032, India

²Indian Association for the Cultivation of Science, Jadavpur, Kolkata 700032, India

(Received 8 May 2013; accepted 13 July 2013; published online 25 July 2013)

The π electron cloud above and below the honeycomb structure of graphene causes each carbon atom to carry a permanent electric quadrupole moment which can attach any cation to impart interesting physical properties. We have synthesized Fe intercalated graphene structures to investigate tunable magnetic properties as a result of this chemical modification. An interesting antiferro quadrupolar ordering is observed which arises due to a coupling between magnetic dipole moment of Fe and electric quadrupole moment on graphene surface. In contrast to antiferromagnetic Neel temperature (T_N), here the ordering temperature (T_Q) increases from 35.5 K to 47.5 K as the magnetic field is raised upto 1 Tesla. © 2013 Author(s). All article content, except where otherwise noted, is licensed under a Creative Commons Attribution 3.0 Unported License. [<http://dx.doi.org/10.1063/1.4816791>]

I. INTRODUCTION

The rare earth compounds with 4f electrons possessing orbital as well as spin degrees of freedom, generally show electric quadrupole ordering in addition to magnetic dipole ordering at low temperatures.^{1,2} Cerium hexaboride (CeB_6) is considered as a typical example of an f-electron system, where Ce^{+3} ions are arranged in the simple cubic lattice and quadrupolar interactions play an important role in its magnetic behavior.^{3,4} In this compound, the anomalous magnetic behavior where the quadrupolar ordering temperature (T_Q) increases with increasing magnetic field in contrast to the ordinary antiferro Neel temperature (T_N) which dies away with increasing field, arises due to coupling between the magnetic dipole and electric quadrupole. Besides CeB_6 , there are very few other compounds like DyB_2C_2 , HoB_2C_2 , TmTe and $\text{PrOs}_4\text{Sb}_{12}$ where antiferro quadrupolar ordering (AFQ) at low temperature has been observed.^{2,5-8}

Although AFQ is observed so far in very few f-electron systems, there are several basic issues which still remain unexplored. For example, the enhancement of T_Q with magnetic field is very poor and whether the effect can be observed in non-f-electron heterogeneous systems in which the interaction takes place between the magnetic dipole situated on the electric quadrupolar surface. Very recently it has been reported that the π electron cloud above and below the honeycomb structure causes each carbon atom to carry a permanent electric quadrupole moment in graphene.⁹ Although few works on magnetic properties in intrinsic graphene^{10,11} as well as composites^{12,13} containing magnetic materials grown on graphene surface have already been reported, the effect of coupling between the magnetic dipole moment and electric quadrupole moment of graphene has not yet been explored. To investigate whether the AFQ ordering is observed when a magnetic atom is placed on the quadrupole rich graphene surface we have synthesized Fe intercalated graphene using graphene oxide to form a layered structure with an interlayer separation of 4.4 Å.

^aE-mail address of Corresponding author: cnssks@iacs.res.in



TABLE I. Compositions for three different Fe intercalated FLG composite.

Sample No.	Amount of GO solution taken	Amount of anhydrous FeCl ₃ taken ('X')
Sample 1 (GF 1)	10 ml	0.006 mol
Sample 2 (GF 2)	10 ml	0.030 mol
Sample 3 (GF 3)	10 ml	0.015 mol

II. EXPERIMENTAL

To synthesize Fe intercalated few layer graphene (FLG) sheets; FLG oxide (FLGO) is prepared from natural purified graphite using modified Hummer's method.¹⁴ 10 ml of FLGO solution is mixed with 100 ml of DMF in a beaker followed by ultrasonic vibration in a cold water bath to yield a clear homogeneous yellow brown dispersion. In a typical process to prepare Fe intercalated FLG composite we have synthesized three samples (GF) with different amounts of anhydrous FeCl₃ as shown in Table I.

Aqueous solution of FeCl₃ is then added to the homogeneous yellow brown dispersion of GO. The mixture is stirred for 30 min and treated by ultrasonic vibration for 15 minutes to make a uniform mixture. Finally, 10 ml of hydrazine hydrate is added to the mixture followed by further ultrasonic treatment for 4 h at a temperature of 60°C. The final product is collected by filtration, washed with distilled water and methanol and then dried in vacuum oven at 80°C overnight.

Transmission electron micrograph (TEM) studies of the as-synthesized samples are performed by Jeol-2011 high resolution transmission electron microscope and subsequently for XRD profile, we have used X-RAY Diffractometer (Rich Seifert). Raman Measurements are carried out using LabSpec Raman spectroscope (Model JYT6400). The sample for Raman measurement was excited at 514 nm with an Ar-ion laser with a scanning duration of 50 s. The XPS measurements are carried out using OMICRON-0571 system. For DFT calculation we have used standard program of GUSSIAN 03 software package. Magnetic measurements have been carried out by SQUID Magnetometer (Quantum Design) over the temperature range from 2-300 K.

III. RESULTS AND DISCUSSION

Fig. 1(a) shows the X-ray diffraction pattern for GF measured at room temperature. From the JCPDS (No. 44-1415) data it is seen that the diffraction peaks for GF sample corresponding to 2θ values of 14.9°, 26.9°, 37.4° and 46.3° can be attributed to the (200), (210), (410) and (020) planes of γ -FeOOH. We have confirmed the Fe intercalation in FLG from the XRD pattern in which a new peak appears at 2θ value of 19.8° corresponding to interlayer separation 4.4 Å, which is close to the theoretical limit (4.0-4.4 Å) of transition metal intercalated graphene layers predicted using DFT technique.¹⁵ Therefore, from the XRD data it is to be mentioned that in this technique during synthesis of Fe intercalated FLG from few layers graphene oxide (FLGO) solution we could not avoid the formation of some γ -FeOOH nanoparticles which grow as a byproduct on top and bottom surfaces but do not affect the properties under investigation. In the previous work¹⁶ we have demonstrated Ni/Graphene/Ni spin valve like structures using Ni layers grown on both sides of graphene sheets. In that case in the first step Ni(OH)₂ was grown during hydrothermal treatment of reduced graphene oxide (RGO) and nickel acetate. In the second step Ni sheets are grown by hydrogen reduction of Ni(OH)₂ at 450°C. However, in the present case we have used ultrasonic vibration to exfoliate the graphene layers for intercalation of transition metal atoms. As a result of this intercalation, in the present work a new peak arises at 19.8° which was absent in the previous work.

From the transmission electron microscope images presented in Fig. 1(b) which is typical of all samples, growth of some discrete γ -FeOOH sheets are also shown. It is to be noted that the major part of the graphene sheet is free from γ -FeOOH. However to give a rough estimate of Fe concentrations we have investigated EDX analysis shown in tabular form of Fig. 1(c).

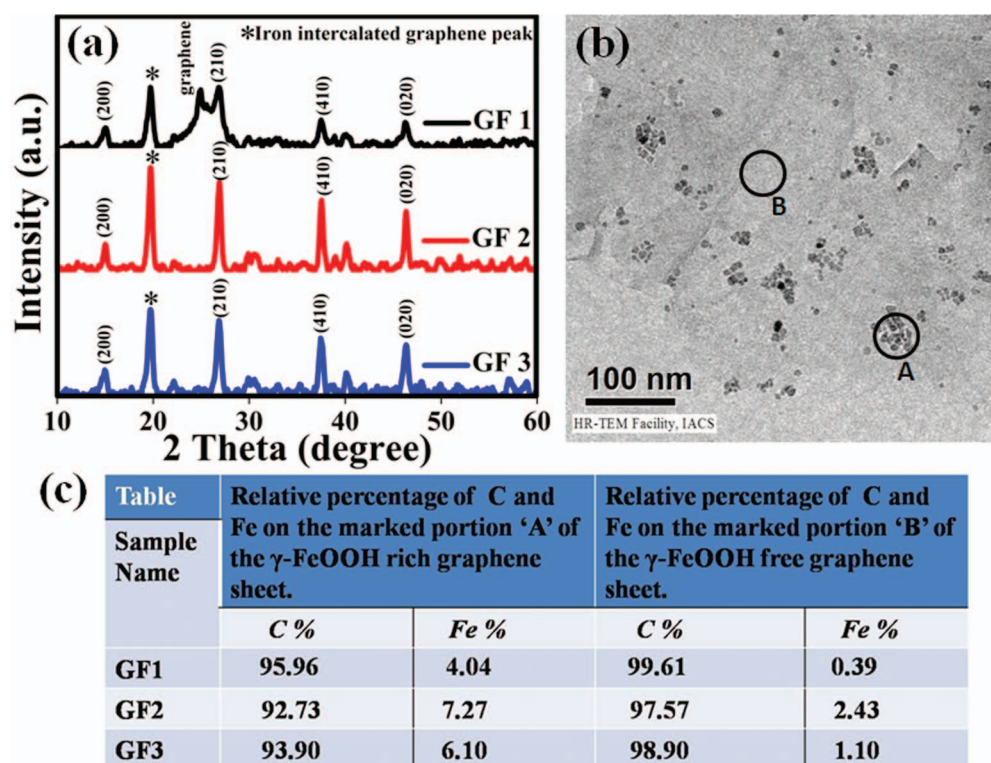


FIG. 1. (a) X-ray diffraction patterns for three samples (GF1, GF2 and GF3) indicating the crystal phase of γ -FeOOH along with Fe intercalated graphene peak. (b) TEM image showing some isolated γ -FeOOH nanoparticles grown on iron intercalated graphene surface. (c) Table reporting the rough estimate of C and Fe concentrations of the three samples as obtained from EDX analysis.

We have performed Raman experiments to understand the number of layers in our Fe intercalated FLG sample. From the literature it is well known that for graphene the peaks corresponding to the 'D' and 'G' bands appear at 1350 and 1580 cm^{-1} and the '2D' band appears at 2700 cm^{-1} . Fig. 2(a) represents the Micro Raman spectra for the as-synthesized sample. In this case the 'D' and '2D' bands appear at 1347 and 2690 cm^{-1} . The interesting observation is the appearance of 'G' band peak, shown in the inset of Fig. 2(a). The G peak appears as a doublet with one peak located at around 1589 cm^{-1} (G_1) and the other at approximately 1597 cm^{-1} (G_2). This doublet in G peak confirms the intercalation and the integrated intensity ratio I_{G1}/I_{G2} close to unity indicates 3 layers in our FLG samples.^{17,18}

To confirm the Fe intercalation we have carried out X-ray photoelectron spectroscopy (XPS) analysis shown in Figs. 2(b) and 2(c). In Fig. 2(b) the peak corresponding to binding energies (B.E.) at about 285 and 531 eV are attributed to C1s and O1s respectively and peaks in the marked portion represents the B.E. of Fe2p. It is seen from enlarged view of Fe2p peaks shown in Fig. 2(c) that the peaks at 711.5 and 725.2 eV correspond to the B.E. of Fe2p_{3/2} and Fe2p_{1/2} in the oxidized state of Fe(III) arising due to the presence of γ -FeOOH. These results are in good agreement with the TEM microstructure and XRD profile where lattice image as well as the peaks corresponding to the γ -FeOOH phase confirms the formation of γ -FeOOH nanosheets on the graphene surface. Besides Fe2p_{3/2} and Fe2p_{1/2} peaks a small and broad peak is also observed at B.E. 706.5 eV. The appearance of this peak at B.E. 706.5 eV shows a clear indication of Fe(0) state which is absent in both the XRD profile as well as in the TEM micrograph.

In this regard, it is to be mentioned that we have thoroughly investigated the high resolution lattice images of the nanocrystallites grown on the graphene surface but no evidence of metallic Fe lattice even in the trace amount is observed. Therefore, from the TEM, XRD, Raman and XPS results it is confirmed that Fe(0) is intercalated in between the graphene layers and a stable structure

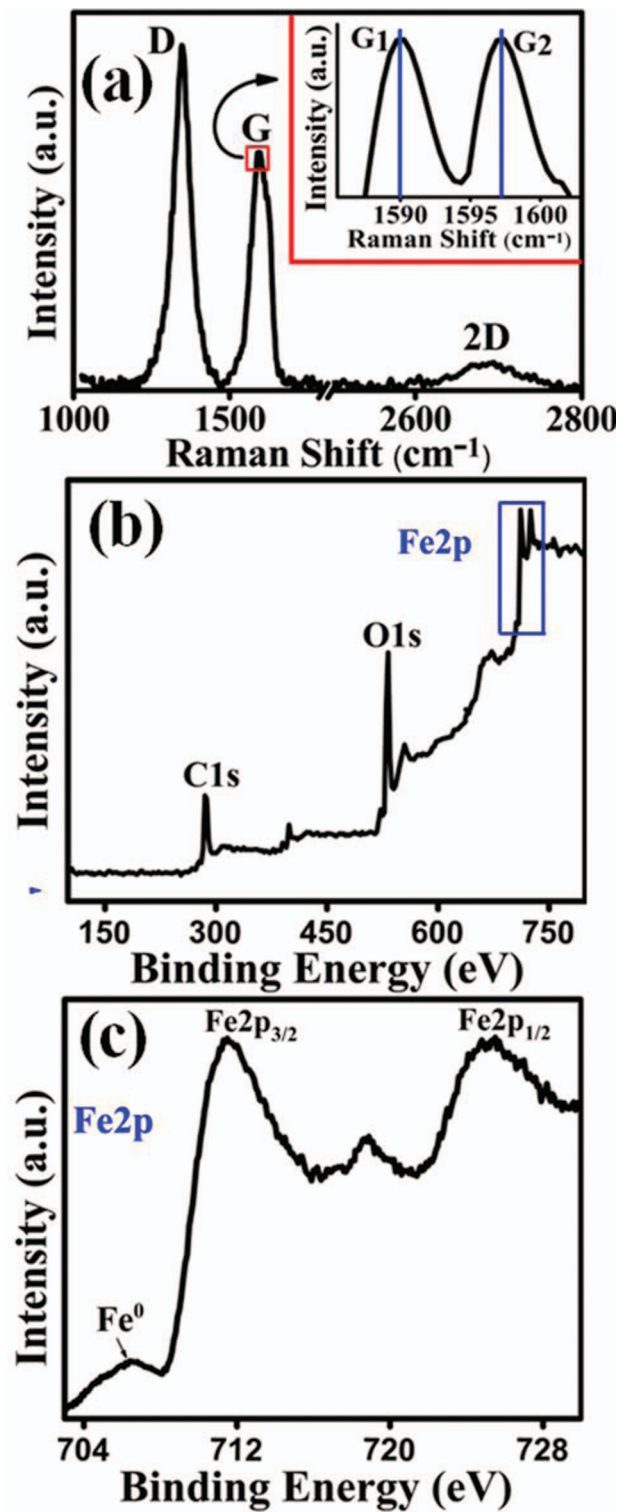


FIG. 2. (a) Raman study for the GF sample. The inset of figure 2 (a) shows the splitting of G peak confirming the intercalation of Fe in graphene and the number of layers present in the Fe intercalated FLG. XPS spectra of GF (b) full survey (c) survey for Fe2p.

is formed due to mixing of d-orbitals of Fe and p-orbitals of carbon discussed later. We have also overruled the existence of Fe(0) on the surface of graphene because of high reactivity of Fe(0) with oxygen to form a stable Fe-oxide phase.

Based on our TEM, XRD, Raman and XPS results we conclude that during the growth process Fe atoms are intercalated within the graphene layers along with the formation of γ -FeOOH on both surfaces of FLG sheets. During synthesis of FLGO by modified Hummer's method we have controlled the oxidation in such a way that it takes place only on two faces along with side edge of a few layer graphene sheets with the formation of epoxy, hydroxyl, and carboxyl groups on their basal planes and edges respectively creating a negatively charged environment and Fe^{3+} ions favorably bind with the oxygen-containing groups when the FLGO solution is stirred in the presence of FeCl_3 . In the first step of sonication before addition of the reducing agent (hydrazine hydrate) Fe^{+3} ions are penetrated in between the graphene layers due to partial exfoliation as a result of steric repulsion between the $-\text{COOH}$ groups attached to the edges and finally when hydrazine hydrate is added under sonication at 60°C , hydrolysis of Fe^{+3} accompanied by the formation of γ -FeOOH occurs on the top and bottom surfaces of FLG and simultaneously the Fe^{+3} ions that penetrated in between the graphene layers are reduced to form metal atom and intercalated due to strong interaction between the d-orbitals of TM atom and p-orbitals of graphene carbon atoms. The as synthesized powdered sample is washed several times using aqueous solution and centrifuge and finally dried in vacuum oven at 90°C for 3h. This results in the fabrication of an intercalated structure with an interlayer separation corresponding to a 2θ value of 19.8° . It is noticed that for lower Fe content (GF1) there is a graphene peak at around 24.8° . It means for lower Fe content some portions still remain to be intercalated. For higher Fe content however, the intercalation is complete as for samples GF2 and GF3 for which no graphene peak at 24.8° is observed.

To investigate the stability of Fe intercalated graphene structure we have also carried out DFT calculation. In case of intercalation when Fe is intercalated in between two graphene sheets, its vibrational energy as well as stabilization energy is accordingly modified. We estimate the total energy and molecular orbital (M.O) calculation of the optimized metal atom intercalated structure with B3LYP/3-21G, 6-31G levels using the standard program of in GUSSIAN 03 software package. We have found that Fe atom intercalated structure is energetically more stable than the Fe atom placed on the top/bottom surfaces of graphene and the intercalated optimized structure shows the lowest energy value of -1084411.675 Kcal/mol in all basis sets for the B3LYP technique. Again the presence of Fe atom on top/bottom surfaces of graphene is discarded from the FE-TEM and XPS experimental results. The difference in energy for the intercalated structure with Fe atom in the centre position as well as off centre position of the graphene ring found to be 71155.1255 Kcal. Therefore, we conclude that it is energetically more favorable for the iron atom to be intercalated at the centre position in between the graphene layers. Also at the same time for the optimized system, the interlayer separation is found to be 4.39 \AA , which is almost well in agreement with our experimental results (4.4 \AA). Fig. 3(a) shows the spin density distribution for the occupied molecular orbital (HOMO-33) and Fig. 3(b) that for the unoccupied molecular orbital (LUMO-115) which are separated by 0.3 eV . The interactions (orbital overlap) of the π electrons of graphene surface (p_z) with the $d\pi$ electrons (d_{z^2}) of iron, shown in Fig. 3(b) is stable owing to its $p\pi$ - $d\pi$ stacked spin topological frameworks.

Fig. 4(a) shows the Field Cooling (FC) with a magnetic field of 500e and zero field cooling (ZFC) curves for the sample (GF1) with lower Fe content. The peak in FC curve of GF1 clearly shows an antiferromagnetic interaction with T_N at around 32.5 K and the Blocking temperature obtained from ZFC curve is about 104.7 K although the splitting in FC and ZFC curves starts almost from room temperature (300 K). To understand the effect of magnetic field on antiferromagnetic interaction we have extended field cooled measurements using a magnetic field of 1 Tesla as shown in Fig. 4(b). Like other antiferromagnetic samples, in the present case also we observe that the antiferromagnetic interaction dies away under the application of a magnetic field of about 1 T .

Striking difference in magnetic behavior for the samples (GF2, GF3) is observed. Fig. 5(a) shows the Field Cooling (FC) with a magnetic field of 500e and zero field cooling (ZFC) curves for GF2 which clearly show an antiferromagnetic interaction with T_N at around 35 K and the Blocking temperature obtained from ZFC curve is about 53.5 K although the splitting in FC and

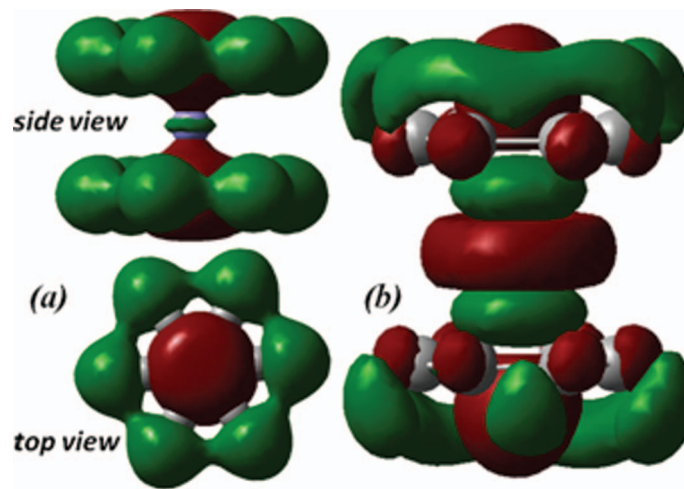


FIG. 3. Spin density distributions of (a) occupied HOMO-33 (side and top view) and (b) unoccupied LUMO-115 (right) molecular orbitals for the optimized iron intercalated graphene structure, calculated using GAUSSIAN 03 with UB3LYP/6-31G method

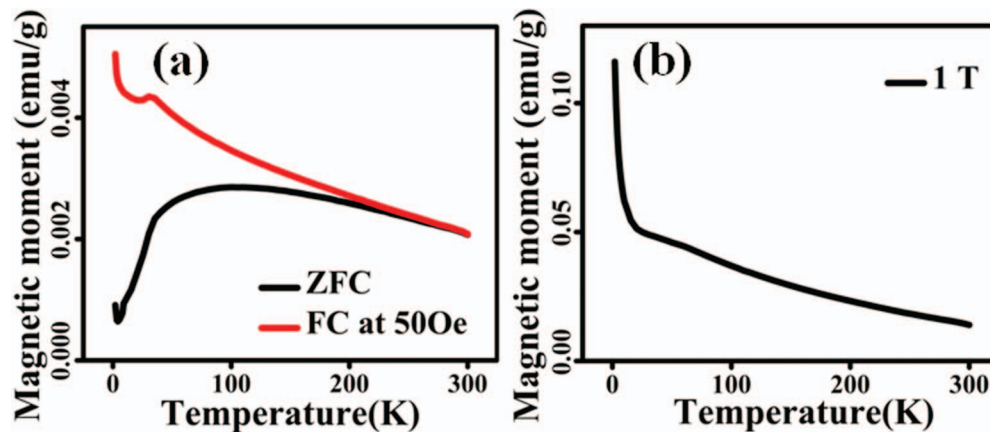


FIG. 4. (a) ZFC-FC curves for GF1 at 50Oe which gives ordinary antiferromagnetic interaction due to γ -FeOOH nanoparticles. (b) FC curve for GF1 at 1 T showing the disappearance of Neel temperature at higher magnetic field.

ZFC curves starts almost from 80 K. To understand the effect of magnetic field on antiferromagnetic interaction we have extended field cooling measurements at different fields as shown in Fig. 5(b). Striking difference in magnetic behavior compared to antiferromagnetic interaction where the peak in FC curve shifts to lower temperature at higher magnetic field is observed. In this case the peak temperature in FC curves shifts to a higher value with increasing magnetic field as shown in Fig. 5(b).

To elucidate this unusual magnetism in Fe intercalated FLG we invoke the antiferro quadrupolar ordering (AFQ) which arises due to the interplay between the magnetic dipole moment of Fe d-electrons and the electric quadrupole moment of carbon p-electrons on the graphene surface. This AFQ ordering is generally observed in very few 4f-electron systems like CeB₆, TmTe etc. however, this is very interesting to explore whether this effect is observable as a result of interaction between the magnetic moment of Fe and the quadrupole rich graphene surfaces within which the Fe is intercalated. To understand this interaction between the d-orbitals of Fe atom with p-orbitals of graphene carbon atoms we have considered the graphene surface as the X-Y plane as shown in Fig. 5(c). In sp² hybridized graphene, all p_z orbitals above and below the graphene plane produces the delocalized π -electrons which create sufficient quadrupole moment on each carbon atom.

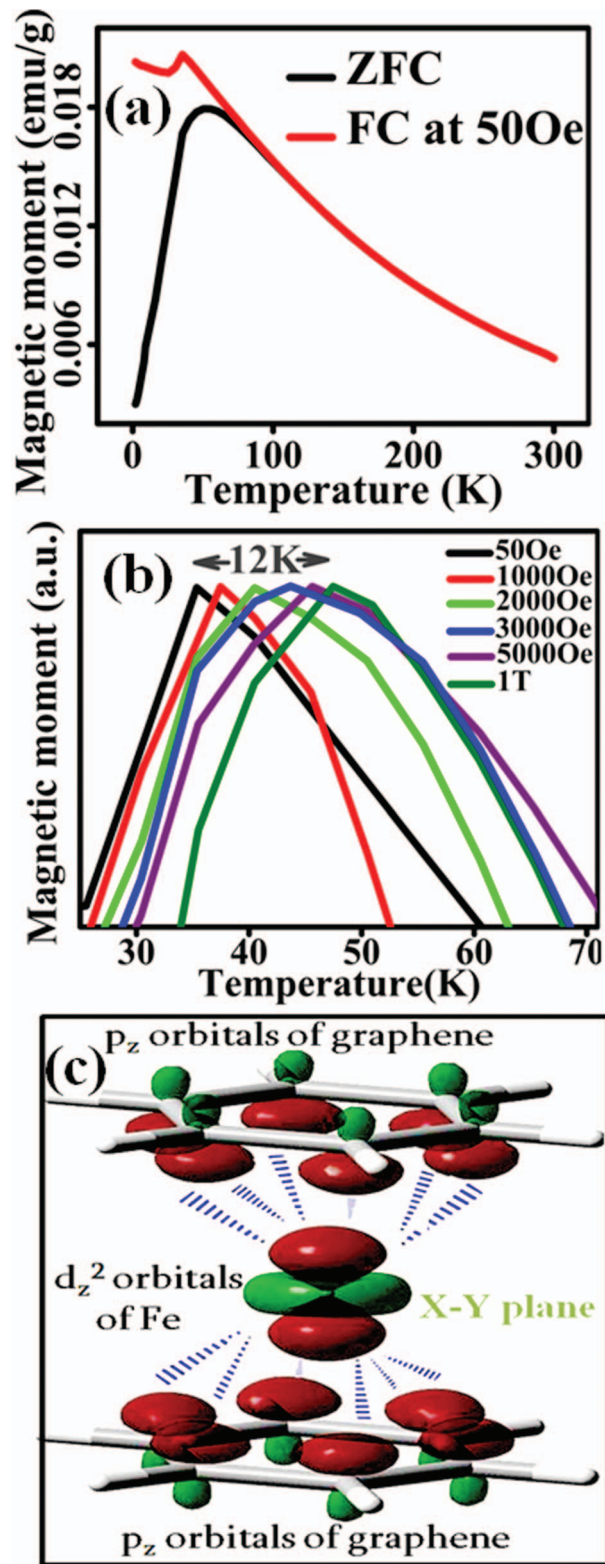


FIG. 5. (a) ZFC-FC curves for GF2 at 500 Oe. (b) Enlarged view of FC curves for GF2 at different fields. The ordering temperature (T_Q) increases from 35.5 K to 47.5 K for a field variation up to 1 T. (c) Schematic representation of the interaction between the intercalated Fe ' d_z^2 ' orbitals with the ' p_z ' orbitals of graphene.

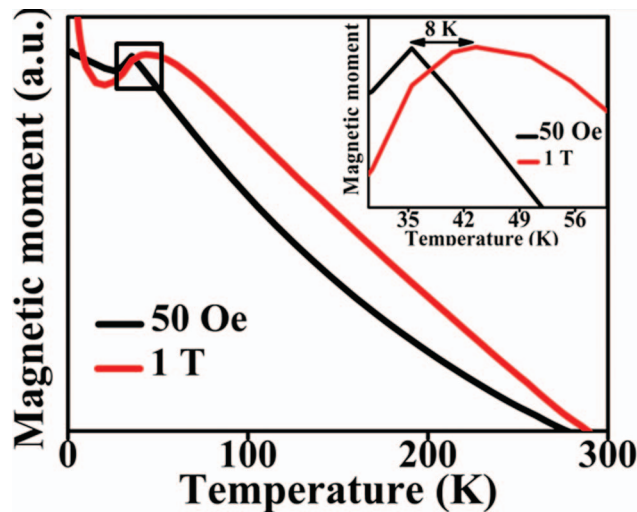


FIG. 6. FC curves for GF3 at 50 Oe and 1 T and the inset shows the enlarged view of the marked region.

Due to interaction with these p_z orbitals, the d-orbitals (d_{xy} , d_{yz} , d_{zx} , $d_{x^2-y^2}$ and d_{z^2}) of intercalated Fe will be modified and the most affected orbital is the d_{z^2} orbital due to axial overlapping. As a result of this strong axial interaction of the d_{z^2} electron carrying an unpaired spin moment with the electric quadrupole moment of the p_z orbital electron, the AFQ ordering is observed in the present Fe intercalated FLG sheets. In this regard it is to be pointed out that from symmetry consideration the d_{z^2} orbital of Fe atom interacts equally with p_z orbitals of all carbon atoms in the ring as shown in Fig. 5(c) and such type of interaction between d-orbital of transition metal and p_z -orbital of carbon is reported in the literature.¹⁹

In GF1, AFQ ordering is not observed because of the lower concentration of Fe atoms. As the value of potential for the quadrupole decreases with 5th power of the distance, the interaction between the magnetic quadrupolar moments induced due to the interplay between the magnetic dipole moment of Fe and electric quadrupolar moment on the graphene surface is too small to observe AFQ for lower concentration of Fe. As a result, the ordinary antiferromagnetic ordering due to magnetic dipole moment of γ -FeOOH with T_N 32.5 K, which dies away with increasing field of 1 T is observed. But for higher concentration (GF2), large numbers of Fe atoms are intercalated between the graphene layers, which essentially diminish the distance between the magnetic quadrupole moments resulting in the AFQ ordering. In contrast to T_N in ordinary antiferromagnetism, the unique feature of this AFQ is that the ordering temperature (T_Q) increases with increasing magnetic field and in our case we have been able to achieve a remarkable shift of T_Q by an amount of 12 K from 35.5 K to 47.5 K for a change in magnetic field of 1 T as shown in Fig. 5(b). Upon further increasing the magnetic field to 3.5 T we do not observe any such shift of transition temperature. Here, we would like to emphasize on two basic issues, one being the observation of AFQ in non f-electron systems and the other is the large shift of T_Q with magnetic field compared to the literature results where a shift of temperature 7 K is observed for a magnetic field of 30 T.

An interesting aspect of the present investigation would be the clustering effect of Fe atoms on AFQ ordering. It is argued, however, that the latter essentially will be suppressed due to comparatively stronger dipole-dipole interaction between Fe atoms. It is therefore concluded that to observe AFQ ordering there should be an optimum concentration of Fe atoms in between the graphene layers. To study this effect with quantitative estimation of Fe atoms a theoretical work is required and such work will be attempted in future. However, to check the effect of Fe content on antiferro quadrupolar ordering, we have carried out magnetic measurements on another sample (GF3) with Fe content intermediate between GF1 and GF2. Fig. 6 shows the FC curves for GF3 at different magnetic field values.

In this case T_Q observed at 35.4 K for 50 Oe and shifts to 43.4 K at 1 T magnetic field. It is to be mentioned that in this case the shift of T_Q is lesser than GF2 due to lower concentration of Fe atoms resulting smaller AFQ ordering compared to GF2.

IV. CONCLUSION

In summary, unusual magnetism in Fe intercalated graphene layers exhibiting antiferro quadrupolar ordering as a result of interplay between the magnetic dipole moment of Fe atom and electric quadrupole moment on the graphene surface is observed. Remarkable shift of ordering temperature (T_Q) with increasing magnetic field compared to the literature results indicates strong interaction between the magnetic moment of Fe atom and quadrupolar moment on the graphene surface.

ACKNOWLEDGMENTS

AJA and AG acknowledge DST, New Delhi and CSIR respectively for awarding the fellowships during the work. DC thanks INSA, New Delhi for giving him a honorary scientist's position. SKS acknowledges DST, New Delhi, Govt. of India for financial support, Project No. SR/NM/NS-1089/2011.

- ¹ T. Yanagisawa, T. Goto, and Y. Nemoto, *Phys. Rev. B* **71**, 104416 (2005).
- ² H. Yamauchi, T. Osakabe, E. Matsuoka, and H. Onodera, *J. Phys. Soc. Jpn.* **81**, 034715 (2012).
- ³ D. Hall, Z. Fisk, and R. G. Goodrich, *Phys. Rev. B* **62**, 84 (2000).
- ⁴ S. W. Lovesey, *J. Phys.: Condens. Matter* **14**, 4415 (2002).
- ⁵ K. Hirota, N. Oumi, T. Matsumura, H. Nakao, Y. Wakabayashi, Y. Murakami, and Y. Endoh, *Phys. Rev. Lett.* **84**, 2706 (2000).
- ⁶ Y. Tanaka, T. Inami, T. Nakamura, H. Yamauchi, H. Onodera, K. Ohoyama, and Y. Yamaguchi, *J. Phys.: Condens. Matter* **11**, L505 (1999).
- ⁷ J.-M. Mignot, P. Link, A. Gukasov, T. Matsumura, and T. Suzuki, *Physica B* **281 & 282**, 470 (2000).
- ⁸ R. Shiina, *J. Phys. Soc. Jpn.* **75**, 114708 (2006).
- ⁹ E. Bichoutskaia and N. C. Pyper, *J. Chem. Phys.* **128**, 024709 (2008).
- ¹⁰ Y. Wang, Y. Huang, Y. Song, X. Zhang, Y. Ma, J. Liang, and Y. Chen, *Nano Lett.* **9**, 220 (2009).
- ¹¹ S. K. Saha, M. Baskey, and D. Majumdar, *Adv. Mater.* **22**, 5531–5536 (2010).
- ¹² M. Weser, Y. Rehder, K. Horn, M. Sicot, M. Fonin, A. B. Preobrajenski, E. N. Voloshina, E. Goering, and Y. S. Dedkov, *Appl. Phys. Lett.* **96**, 012504 (2010).
- ¹³ C. V. Van, S. Schumacher, J. Coraux, V. Sessi, O. Fruchart, N. B. Brookes, P. Ohresser, and T. Michely, *Appl. Phys. Lett.* **99**, 142504 (2011).
- ¹⁴ W. S. Hummers and R. E. Offeman, *J. Am. Chem. Soc.* **80**, 1339 (1958).
- ¹⁵ T. P. Kaloni, M. U. Kahaly, and U. Schwingenschlogl, *J. Mater. Chem.* **21**, 18681 (2011).
- ¹⁶ S. Mandal and S. K. Saha, *Nanoscale* **4**, 986 (2012).
- ¹⁷ D. Zhan, L. Sun, Z. H. Ni, L. Liu, X. F. Fan, Y. Wang, T. Yu, Y. M. Lam, W. Huang, Z. X. Shen, *Adv. Funct. Mater.* **20**, 3504 (2010).
- ¹⁸ M. H. Dresselhaus and G. Dresselhaus, *Adv. Phys.* **51**, 1 (2002).
- ¹⁹ N. Atodiresei, J. Brede, P. Lazic, V. Caciuc, G. Hoffmann, R. Wiesendanger, and S. Blügel, *Phys. Rev. Lett.* **105**, 066601 (2010).